Pakistan Veterinary Journal

ISSN: 0253-8318 (PRINT), 2074-7764 (ONLINE)
DOI: 10.29261/pakvetj/2026.185

RESEARCH ARTICLE

Temporal Analysis of the Immune Response Following Single Subcutaneous Bacillus Calmette–Guérin Vaccination in C57BL/6 Mice

Eun Bee Choi[1†], Ye Jin Yang[2†], Kwangwook Kim[1], Seo Young Moon[1], Heeji Lim[1], Yoo-Kyung Lee[1], In-Ohk Ouh[1]* and Kwang Il Park[2]*

[1]Division of Vaccine Development Coordination, Center for Vaccine Research National Institute of Infectious Diseases, Korea National Institute of Health, Korea Disease Control and Prevention Agency, Cheongju-si 28159, Republic of Korea; [2]Department of Veterinary Physiology, College of Veterinary Medicine of Gyeongsang National University, Gazwa, Jinju 52828, Republic of Korea. † These authors contributed equally to this work.
*Corresponding author: dvmoio@korea.kr (I.O.O.), kipark@gnu.ac.kr (K.I.P.)

ARTICLE HISTORY (26-115)

Received: February 12, 2026
Revised: August 17, 2026
Accepted: August 19, 2026
Published online: August 22, 2026

Key words:
Bacillus Calmette–Guérin
C57BL/6 mouse
Mycobacterium tuberculosis
Tuberculosis

ABSTRACT

Bacillus Calmette–Guérin (BCG) is the only licensed vaccine against tuberculosis (TB); however, the temporal dynamics of post-vaccination immunity have not been fully established. We examined systemic and tissue-specific immune responses at 4, 6, and 8 weeks following BCG immunization in C57BL/6 mice. Serum cytokine analysis revealed progressive increases in IFN-γ and IL-2, with the highest concentrations observed at week 8. In contrast, ELISpot analysis indicated that IFN-γ-producing splenocytes peaked at week 4 and subsequently decreased, although their numbers remained significantly higher at weeks 6 and 8 compared with the unvaccinated controls. Lung-derived immune cells showed a modest increase in IFN-γ-producing cells at later time points; however, these differences did not reach statistical significance. Gene expression analysis revealed significant late-stage increases in IFN-γ and CXCL10 transcripts in lung tissue, which indicated enhanced local Th1-associated transcriptional activity. Histological examination revealed immune activation without marked tissue pathology, whereas immunohistochemical (IHC) analysis showed time-dependent changes in cytokine-positive cells in the spleen and lung. Following aerosol challenge with *Mycobacterium tuberculosis* (M.tb), mice vaccinated for 6 or 8 weeks exhibited reduced pulmonary bacterial burden, with the greatest reduction observed in the 8 weeks group at later post-challenge time points. Taken together, these results demonstrate that BCG-induced immunity exhibits distinct assay- and tissue-specific kinetics, characterized by an early splenic cellular response, followed by later systemic and pulmonary immune activation. This integrated temporal analysis provides useful insight for selecting assessment time points in preclinical BCG studies.

To Cite This Article: Choi EB, Yang YJ, Kim KW, Moon SY, Lim HJ, Lee YK, Ouh IO and Park KI, 2026. Temporal analysis of the immune response following single subcutaneous Bacillus Calmette–Guérin Vaccination in C57BL/6 mice. Pak Vet J, 46(8): 2004-2015. http://dx.doi.org/10.29261/pakvetj/2026.185

INTRODUCTION

Tuberculosis (TB) is an infectious disease caused by *Mycobacterium tuberculosis* (M.tb), which is primarily transmitted through airborne particles containing tubercle bacilli (Bussi and Gutierrez, 2019; Furin *et al.*, 2019). Following inhalation of these aerosolized bacilli, the respiratory tract, particularly the lungs, is the primary site of infection (Lyon and Rossman, 2017). The host immune response isolates the bacterium as a latent infection when it occurs in the new host (Chee *et al.*, 2018); however, the afflicted individual suffers the infectious and active phase of the illness if there is coinfection or immunological suppression (Fatima *et al.*, 2020). Following pulmonary infection, M.tb is primarily phagocytosed by alveolar macrophages and dendritic cells (Sankar and Mishra, 2023). The recruitment and organization of infected macrophages and other immune cells, including lymphocytes, contribute to the formation of granulomas, which are a characteristic pathological feature of TB (Suarez *et al.*, 2019; Sawyer *et al.*, 2023). Although granulomas restrict bacterial dissemination, they also provide a specialized microenvironment in which M.tb persists (Cho *et al.*, 2021). The bacterium promotes

intracellular survival by interfering with host antimicrobial mechanisms, such as phagosome maturation, lysosomal degradation, and autophagic pathways (Cho *et al.*, 2021). Consequently, M.tb can remain within the host for prolonged periods and may become reactivated when host immune control is weakened (Bussi and Gutierrez 2019; Warner *et al.*, 2025). Thus, the immunological status of the host is a major determinant of TB progression and disease severity (Cho *et al.*, 2021).

Bacillus Calmette–Guérin (BCG) is the only vaccine available to treat TB (Ritz *et al.*, 2008). It is the most commonly used vaccine and a strong immune response modulator (Bickett *et al.*, 2020; Kowalewicz-Kulbat and Locht, 2021). Over 120 million doses are administered each year (Ritz *et al.*, 2008; Mata *et al.*, 2021). BCG is a live attenuated TB vaccine that induces non-specific cross-protection against pathogens that may be unrelated to the target disease and was first used in 1921 (Foster *et al.*, 2021; Chen *et al.*, 2023). BCG vaccination reduces the mortality of newborns and induces an improved innate immune response against microorganisms other than M.tb, such as *Candida albicans* and *Staphylococcus aureus* (Covian *et al.*, 2019).

Among all animal models used in TB research for testing vaccine candidates, drugs targeting TB, and protective immunity induced by BCG immunization, mice are the preferred choice (Ritz *et al.*, 2008; Khatri *et al.*, 2021). Mouse models are widely used because of their small size, relatively low cost, and wide availability (Khatri *et al.*, 2021). Through published TB challenge studies (Kramnik and Beamer, 2016), BCG protective responses against TB in mice have been shown to vary with respect to mouse strain (Coppola *et al.*, 2021), strains of M.tb. for infection, route of immunization for BCG vaccination, and M.tb. challenge (Khatri *et al.*, 2021).

In this study, we determined the long-term immunological effects following BCG vaccination and their effect on immune responses and protective efficacy using an established murine model. The results establish a time period for the BCG vaccine and evaluate the protective responses for an accurate BCG period in mice.

MATERIALS AND METHODS

Animal: Female C57BL/6 (5-week-old) mice were obtained from Samtako (Osan, Republic of Korea). The mice were maintained under specific pathogen-free conditions and fed autoclaved food and water *ad libitum*. The animal facility was maintained at 23 ± 1 °C and 60 ± 5% relative humidity under a 12-h light/12-h dark cycle. Groups of at least five mice were used in all experiments. Each experimental group consisted of 10 mice. Tissue samples from five mice per group were used for histological analyses. Three independent biological samples per group were used for quantitative and statistical analyses (n=3). Before the experiments, the mice were acclimatized for a week in the animal facility.

Ethics for Animal Studies: This study was conducted in agreement with European and national directives for the protection of experimental animals. The experimental procedures were approved by the Ethics Committee for Animal Experiments of Gyeongsang National University (GNU-221024-M0145).

Animal Experiments: The study was divided into two parts: 1) Immunogenicity evaluation: cellular immune responses were analyzed using IFN-γ ELISpot and multiplex cytokine and chemokine assays in BCG-vaccinated and control mice; and 2) H37Rv challenge for different periods of BCG (4, 6, and 8 weeks) vaccination was evaluated by measuring M.tb burden in the lungs and spleen of mice infected with either of the M.tb strains (Fig. 1).

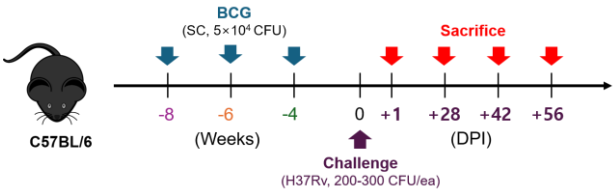

Fig. 1: Experimental design and timeline of BCG vaccination and *Mycobacterium tuberculosis* (M.tb) challenge. C57BL/6 mice were administered a single subcutaneous dose of BCG (5×10^4 CFU) at 8, 6, or 4 weeks before aerosol challenge with M. tuberculosis H37Rv. Vaccinations were staggered so that all groups were challenged simultaneously on Day 0. Following aerosol challenge (approximately 200–300 CFU/animal), mice were sacrificed at DPI 1, 28, 42, and 56 for subsequent analyses. Tissues, serum, and splenocytes were collected for immunological, molecular, and histopathological analyses.

BCG Culture and Preparation: *Mycobacterium bovis* BCG Pasteur $1173P_2$, provided by the Center for Korea National Institute of Health, Korea Disease Control and Prevention Agency (Cheongju-si, Republic of Korea) were cultured on Middlebrook 7H10 agar at 37°C for 2–3 weeks. Colonies were first inoculated into 10 mL of Middlebrook 7H9 broth containing 10% OADC and 0.05% Tween 80 and maintained for 1 week to prepare seed cultures. These seed cultures were then transferred into 400 mL of the same supplemented Middlebrook 7H9 medium and cultured for a further 1 week. Bacterial cells were collected when the culture reached an optical density of 0.7–0.9. To minimize clumping, the suspension was filtered through a 10 µm cell strainer. The bacteria were subsequently washed with 10 mL of 1× PBS by centrifugation at 3,000 rpm for 10 min. After removal of the supernatant, the pellet was resuspended in 8 mL of Middlebrook 7H9 broth supplemented with 10% OADC and 0.05% Tween 80, followed by the addition of 2 mL of 20% glycerol. The resulting suspension was divided into 1 mL aliquots and stored at −70°C until further use. On the following day, one frozen aliquot was thawed and serially diluted in PBS from 10^3 to 10^7. For each dilution, 6–7 drops were plated onto Middlebrook 7H10 agar and incubated at 37°C. Plates were examined over a period of 2–3 weeks, after which visible colonies were enumerated and the viable bacterial concentration was calculated as colony-forming units (CFU).

Experimental Infection: A 3 mL aliquot of the bacterial suspension was loaded into a glass nebulizer-Venturi (Glas-col). Aerosol infection was carried out using the operating conditions listed in Table 1. The aerosol generated was transferred to a whole-body exposure chamber, which operates based on a principle similar to that of the Madison infection chamber. It allows viable bacilli to be deposited in the lungs of mice. Separate

cohorts of mice received a single subcutaneous vaccination with BCG Pasteur 1173P_2 at a dose of 5×10^4 CFU at 8, 6, or 4 weeks before aerosol challenge. To ensure that all vaccinated groups were challenged on the same day, the 8, 6, and 4 weeks groups were vaccinated sequentially in reverse chronological order. All groups were simultaneously challenged with M.tb H37Rv by aerosol exposure at approximately 3×10^2 CFU/mL. The mice were euthanized on day 1 or 4, 6, and 8 weeks after challenge, corresponding to days post-infection (DPI) of 1, 28, 42, and 56, respectively. Initial bacterial burdens in the lungs and spleen were determined in a separate group of C57BL/6 mice euthanized one day after aerosol challenge. These values were used as the baseline for comparison with later time points.

Table 1: Glas-col condition

Step	Function	Time
1	Pre-heating	15 min
2	Nebulizer	30 min
3	Cloud decay	30 min
4	UV	15 min
5	Cool down	10 min
6	END	-

Enzyme-Linked Immunosorbent Assay: Circulating IFN-γ, IL-2, and TNF-α concentrations were quantified in serum samples as indicators of the immune response to BCG immunization. Cytokine concentrations were determined using ELISA kits specific for IL-2 (DY410-05), TNF-α (DY485-05), and IFN-γ (DY402-05) (R&D Systems, USA), following the procedures provided by the manufacturer.

IFN-γ Enzyme-linked Immunospot Assay (ELISpot): After BCG vaccination (4, 6, and 8 weeks), lung cells and splenocytes were isolated from mice, plated in duplicate (lung cell; 2.5×10^5 cells/well and spleen cell; 5×10^5), and incubated at 37°C for 24 h with 10% FBS-RPMI (negative control), protein derivative (PPD) (10 μg/mL), or Ag85B (at a final concentration of 5 μg/mL) or eBioscience cell stimulation cocktail (as a positive control). After 24 h, the number of spot-forming cells (SFCs) was measured using a BD Mouse IFN-γ ELISpot kit (551083) following the manufacturer's instructions. SFCs in each well were automatically enumerated using an ImmunoSpot Micro Analyzer. Net SFCs were calculated by subtracting background values from unstimulated control wells and are expressed as the average number of SFCs per 10^6 splenocytes.

Quantitative PCR: Total RNA was isolated from lung and spleen tissues with the RNeasy Mini Kit (Qiagen, Hilden, Germany). The extracted RNA was then reverse-transcribed to complementary DNA using a reverse transcription kit according to the supplier's protocol. Quantitative PCR analysis was performed with Power SYBR™ Green PCR Master Mix (Thermo Fisher Scientific, USA) on a 7500 Fast Real-Time PCR System (Applied Biosystems). The oligonucleotide primer sequences used for amplification are provided in Table 2. Relative transcript abundance was determined by the $2^{-\Delta\Delta CT}$ method, using β-actin as the internal reference gene for normalization (Zhu *et al.*, 2026).

Table 2: Primer sequences

Gene	Forward	Reverse
TNF-α	TGAACTTCGGGGTGATCG	GGGCTTGTCACTCGAGTTTT
TGF-β	CTCCCGTGGCTTCTAGTGC	GCCTTAGTTTGGACAGGATCTG
IFN-γ	AGAGCCAGATTATCTCTTTCTACCTCAG	CCTTTTTCGCCTTGCTGTTG
IL-6	CTGCAAGAGACTTCCATCCAG	AGTGGTATAGACAGGTCTGTTGG
IL-10	CTTACTGACTGGCATGAGGATCA	GCAGCTCTAGGAGCATGTGG
IL-12	CCAAATTACTCCGGACGGTTCAC	CAGACAGAGACGCCATTCCACAT
IL-17	CTCAAAGCTCAGCGTGTCCAAACA	TATCAGGGTCTTCATTGCGGTGGA
IL-1β	GCTGAAAGCTCTCCACCTCAATG	TGTCGTTGCTTGGTTCTCCTTG
IL-2	GACACTTGTGCTCCTTGTCA	TCAATTCTGTGGCCTGCTTG
CXCL10 (IP-10)	ATCATCCCTGCGAGCCTATCCT	GACCTTTTTTGGCTAAACGCTTTC
β-actin	TGTCCACCTTCCAGCAGATGT	AGCTCAGTAACAGTCCGCCTAGA

Hematoxylin and Eosin Staining: Mouse lung and spleen tissues were fixed in 10% buffered formalin for 24–48 h at room temperature and embedded in paraffin. Each block was cut into 5–8 μm-thick sections using a microtome. The sections were deparaffinized using xylene and ethanol and stained with hematoxylin and eosin. Relative lesion burden was determined using a scoring system (Table 3). Histopathological lesion scoring was performed by an investigator blinded to the experimental group assignments.

Table 3: Histopathological inflammation scoring criteria

Score	Grade	Description
0	Normal	No inflammatory lesions or histological abnormalities
1	Minimal	Minimal focal inflammatory cell infiltration without disruption of normal tissue architecture
2	Slight	Mild focal or multifocal inflammatory cell infiltration involving a limited area of the tissue
3	Moderate	Moderate multifocal inflammatory cell infiltration with partial disruption of tissue architecture
4	Marked	Marked and extensive inflammatory cell infiltration with substantial tissue involvement and structural alteration
5	Severe	Severe diffuse or coalescing inflammation involving most of the tissue, accompanied by extensive tissue destruction, consolidation, or necrosis

Immunohistochemical (IHC) Staining: Lung and spleen specimens were immersed in 4% paraformaldehyde for fixation, processed for paraffin embedding, and cut into 3-μm-thick sections. The sections were then deparaffinized and rehydrated, after which antigen retrieval was carried out by microwave treatment in 10 mM sodium citrate buffer (pH 6.0). Endogenous peroxidase activity was quenched with 3% H_2O_2, and non-specific antibody binding was minimized by incubation with 5% BSA. Primary antibodies were applied to the sections and incubated overnight at 4 °C. Afterward, the sections were incubated with the appropriate secondary antibodies for 2 h. Immunoreactive signals were developed with DAB, followed by hematoxylin counterstaining. Images were captured using a Leica light microscope under identical imaging conditions. For each marker, the color threshold was established using representative images and then applied consistently to all images. Staining intensity was evaluated using the scoring system listed in Table 4. The positively stained area was measured using ImageJ and

expressed as a percentage of the total tissue area. Five randomly selected, non-overlapping fields per tissue section were analyzed from three mice per group. Image quantification was conducted by a researcher blinded to the experimental group assignments.

Table 4: Scoring system for staining intensity

Score	Staining Intensity
0	Absent
1	Low positive signal
2	Moderately strong positive signal
3	Strong positive signal

Growth Inhibition Assay: The assays were conducted by co-culturing lung cells and splenocytes from BCG-vaccinated and M.tb-infected C57BL/6 mice. For the assay, the lung and spleen were the target for M.tb H37Rv infection. Upon termination of the experiment post-challenge, the mice were necropsied, and the spleen and lungs were removed and homogenized using a gentle MACS. 7H10 agar plates were prepared. Stock bacteria stored at −70°C were thawed, diluted to 10^3–10^7, and plated at 2–3 plates per dilution ratio. Serially diluted samples were plated in duplicate onto dried 10% OADC-supplemented 7H10 agar plates. The plates were sealed and incubated at 37°C. The bacterial colonies formed were counted at weekly intervals for 3 weeks. CFU enumeration was conducted by a researcher who was blinded to the experimental group assignments.

Statistical Analysis: Quantitative results are expressed as mean ± SEM. Depending on the experimental design, group differences were evaluated by either one-way or two-way ANOVA. When one-way ANOVA was applied, comparisons were made between each treatment group and the predefined control using Dunnett's post hoc multiple-comparison procedure. Statistical significance was determined based on the adjusted P values generated from this test. All analyses were carried out in GraphPad Prism 8 (GraphPad Software, San Diego, CA, USA). Differences were regarded as statistically significant when the adjusted P value was below 0.05. Where available, the corresponding exact adjusted P values are provided in the figures.

RESULTS

BCG Vaccination Induces a Gradual Increase in Systemic Cytokine Responses: To determine effects of BCG vaccination on systemic immune activation, cytokine levels were measured at defined time points post-vaccination. IFN-γ and IL-2 concentrations increased over time, with the highest levels detected at week 8 (IFN-γ; 35.28 pg/ml; P<0.001, IL-2; 13.63 pg/ml; P=0.012), thus demonstrating a delayed but robust systemic activation (Fig. 2A, B). TNF-α (753.57 pg/mL at 8 weeks) exhibited mild fluctuations without statistical significance, suggesting a supportive but not dominant contribution to systemic immune stimulation (Fig. 2C). Overall, in the C57BL/6 animal model following BCG vaccination, the expression of IFN-γ and IL-2 increased over time, and TNF-α expression was increased at weeks 6 and 8 compared with the control group. Thus, the temporal pattern indicates that BCG does not generate an immediate inflammatory response but rather establishes a progressively maturing immune environment over several weeks. Altogether, these results support the concept that systemic cytokine engagement is observed at later post-vaccination time points.

BCG Vaccination Induces an Early Peak in Splenic PPD-Responsive IFN-γ–Secreting Cells: IFN-γ ELISpot analysis indicated that BCG vaccination induced a robust antigen-specific cellular immune response in C57BL/6 mice. In splenocytes, stimulation with purified PPD significantly increased the number of IFN-γ–producing cells in all vaccinated groups compared with the unvaccinated controls. The splenic IFN-γ response reached its peak at week 4 following vaccination (61.17 SFU/5×10^5; P<0.001) and remained significantly elevated at week 6 (53.84 SFU/5×10^5; P<0.001) and 8 (43.67 SFU/5×10^5; P<0.001), although a gradual decline in magnitude was observed over time (Fig. 3A, C). In lung-derived immune cells, the number of IFN-γ–producing cells was consistently lower compared with that in the spleen but tended to increase in vaccinated mice relative to controls (9.78 SFU/5×10^5 at 8week PPD group) (Fig. 3C). A modest enhancement of IFN-γ responses in the lung was observed with prolonged vaccination; however, these differences did not reach statistical significance (Fig. 3B, D). Notably, the temporal pattern of the splenic ELISpot response differed from the serum IFN-γ profile. PPD-responsive IFN-γ–secreting splenocytes peaked at week 4 and subsequently declined, whereas circulating IFN-γ concentrations increased progressively and were highest at week 8 (Fig. 2). These results indicate distinct kinetics between the frequency of antigen-responsive splenic cells and circulating cytokine concentrations.

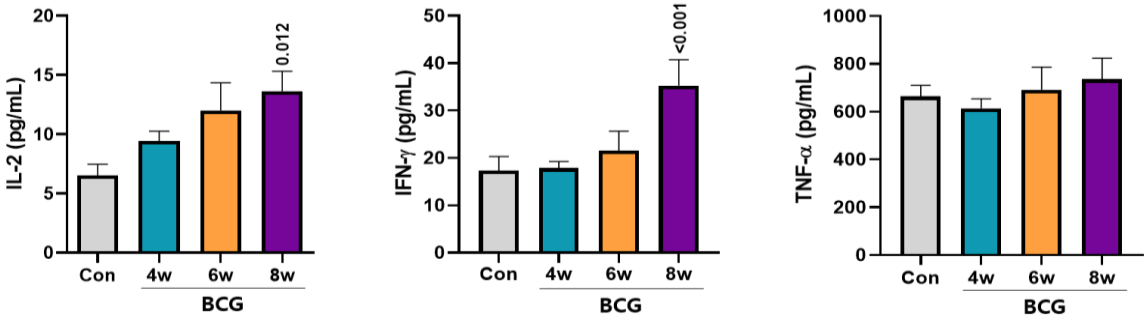

Fig. 2: Serum Cytokine Responses Following BCG Vaccination. Serum levels of IFN-γ, IL-2, and TNF-α were measured in the control group and in the BCG-vaccinated groups at 4, 6, and 8 weeks after vaccination. Data are presented as the mean ± SEM (n=3). Statistical analysis was conducted using a one-way ANOVA followed by Dunnett's multiple comparisons test, with each vaccinated group compared with the control group. Exact adjusted *P* values are shown in the figure.

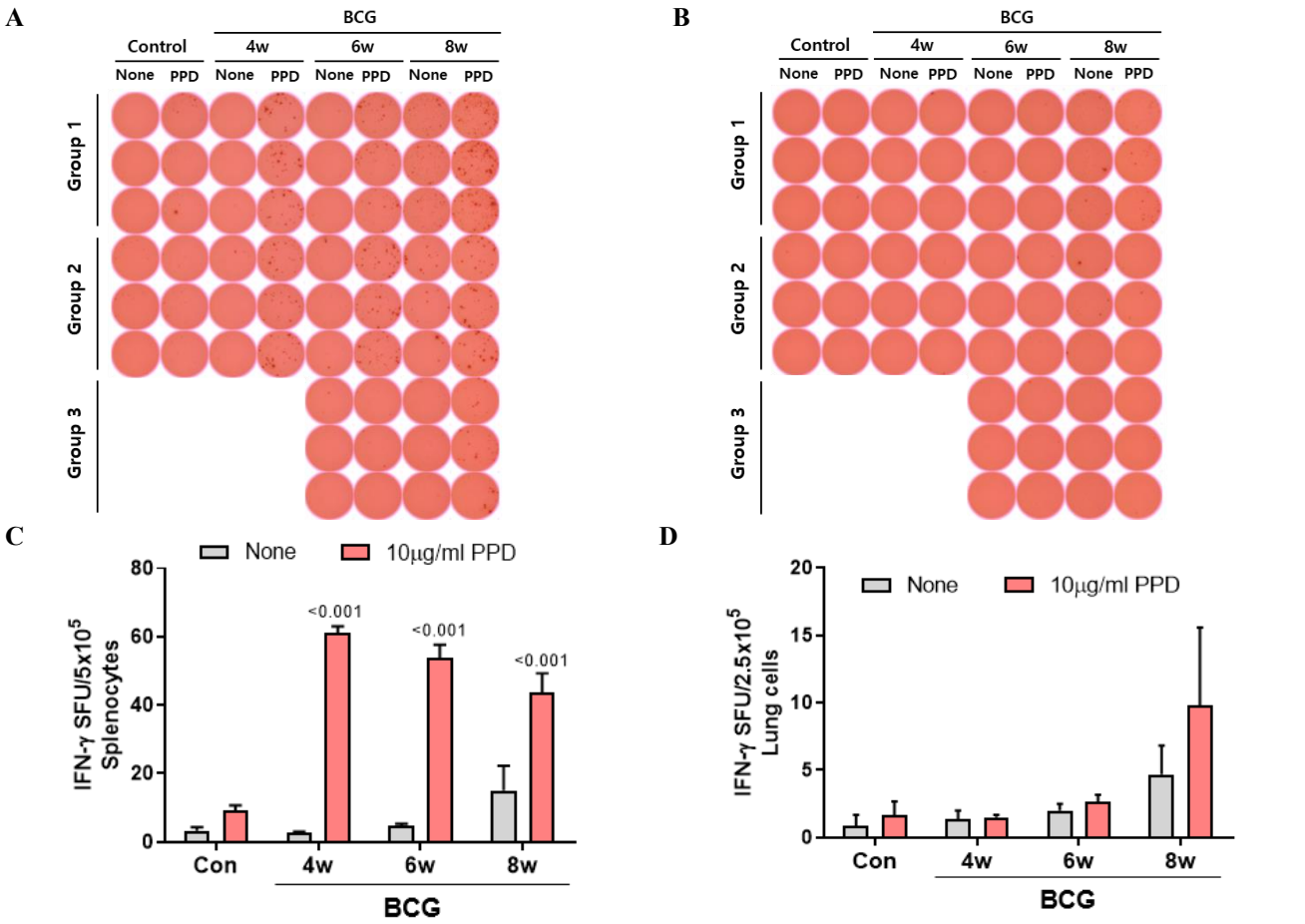

Fig. 3. Functional IFN-γ-secreting cells were assessed using the ELISpot assay. Representative ELISpot images of IFN-γ-secreting cells in (A) splenocytes (5×10^5 cells/well) and (B) lung-derived immune cells (2.5×10^5 cells/well) following stimulation with protein derivative (PPD) (10 μg/mL) for 24 h. Quantitative analyses of IFN-γ-secreting cells are shown for (C) splenocytes and (D) lung-derived immune cells. The data are presented as the mean ± SEM (n=3). Statistical analysis was performed using a one-way ANOVA followed by Dunnett's multiple comparisons test, with each vaccinated group compared with the control group. Exact adjusted *P* values are shown in the figure.

Transcriptional Profiling Reveals Time-dependent Activation of Immune Pathways: To examine the time-dependent changes in immune-related gene expression following BCG vaccination, spleen and lung tissues were collected at 4, 6, and 8 weeks post-vaccination. The expression of TNF-α, TGF-β, IL-17, IL-12, IL-10, IL-6, IL-2, IL-1β, IFN-γ, and CXCL10 mRNA was quantified by real-time PCR (Fig. 4A, B). In the spleen, distinct temporal expression patterns were observed among the genes (Fig. 4A). TNF-α expression was significantly increased at 6 (1.52) and 8 (1.43) weeks compared with 4 weeks (1.22). TGF-β exhibited a modest increase (2.24) at 6 weeks, but no significant differences were detected between time points. IL-2 (1.38), IL-17 (1.86), and IL-12 (1.38) reached peak expression at 4 weeks, and IL-17 was significantly higher at 4 weeks compared with that at 6 and 8 weeks. No significant differences were observed between 6 and 8 weeks for these genes. IL-10 expression was highest at 4 weeks (0.95) and significantly decreased at 6 (0.39; P=0.011) and 8 (0.47; P=0.02) weeks. IL-6 exhibited a decreasing trend without statistical significance. IL-1β was increased at later time points, with IL-1β showing a significant increase at 8 weeks (2.05; P<0.001) compared with 4 weeks (1.06). IFN-γ and CXCL10 exhibited pronounced late-stage upregulation. IFN-γ was significantly increased at 8 weeks (4.22; P<0.001) compared with 4 (1.91; P=0.041) and 6 (1.55) weeks, whereas CXCL10 was significantly increased at 8 weeks (3.61; P<0.001) compared with 4 weeks (2.40; P=0.002). In the lung, gene expression changes were more consistent and sustained over time (Fig. 4B). TNF-α and TGF-β showed an increasing trend, but did not reach statistical significance. IL-12 and IL-17 expression gradually increased; however, no statistically significant differences were observed among the groups. IL-10 expression varied among the groups, with relatively higher levels at 4 (2.24) and 8 (2.59) weeks, whereas IL-6 expression increased primarily at 6 (2.43) and 8 (2.35) weeks. IL-2 also exhibited a gradual increase over time. IL-1β expression peaked at 6 weeks (3.61) and subsequently decreased after 8 weeks (2.1). IFN-γ expression progressively increased from 4 (2.62) to 8 (6.62) weeks, and CXCL10 expression exhibited a marked increase at 8 weeks (7.22); however, no statistically significant differences were observed among the groups. Overall, BCG vaccination produced distinct temporal expression patterns in the spleen and lung. In the spleen, the gene expression changes followed a stepwise pattern, with early and intermediate immune regulation and increased IFN-γ and CXCL10 expression at later time points. In contrast, the lung showed a sustained late-phase response, characterized by significant upregulation of cytokine and chemokine genes.

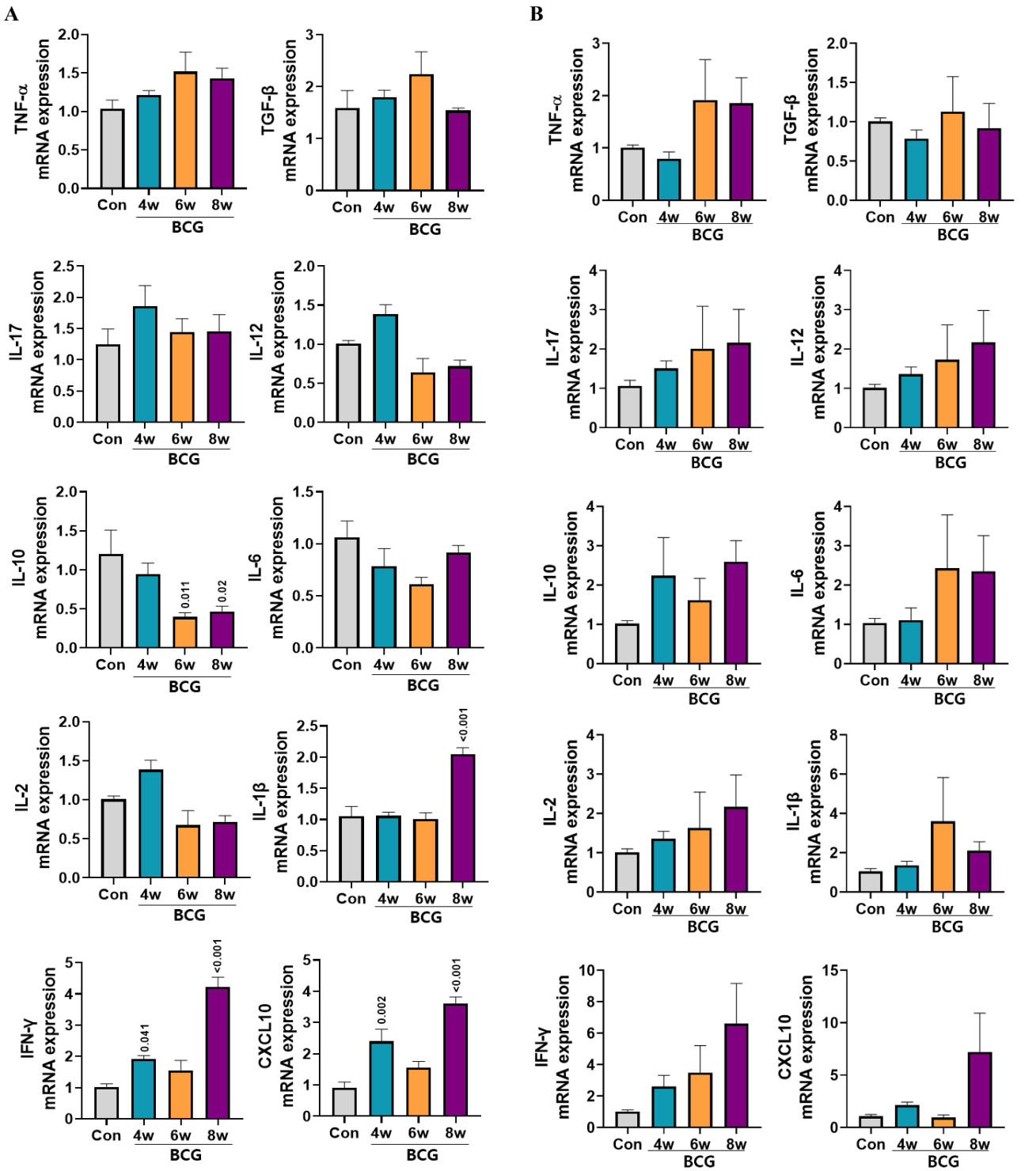

Fig. 4. Cytokine and chemokine gene expression profiles following BCG vaccination. Relative mRNA expression levels of immune-related cytokines and chemokines were determined in (A) spleen and (B) lung tissues collected at 4, 6, and 8 weeks following BCG vaccination. The expression of TNF-α, TGF-β, IL-17, IL-12, IL-10, IL-6, IL-2, IL-1β, IFN-γ, and CXCL10 was quantified by real-time quantitative PCR and normalized to an internal reference gene. The data are presented as the mean ± SEM (n=3). Statistical analysis was performed using a one-way ANOVA followed by Dunnett's multiple comparisons test, with each BCG-vaccinated group compared with the control group. Exact adjusted *P* values are shown in the figure.

Temporal Patterns of Immune Gene Expression in Lung and Spleen Tissues: Heatmap analysis revealed distinct tissue- and time-dependent patterns of cytokine and chemokine expression following BCG vaccination. In the spleen, most immune-related genes exhibited relatively modest and variable changes throughout the vaccination periods, although TNF-α and TGF-β expression increased at week 8 (Fig. 5A). In contrast, lung tissue showed more pronounced temporal changes (Fig. 5B). IFN-γ and CXCL10 expression markedly increased at week 8, whereas IL-12, IL-17, and TNF-α exhibited modest increases over time. IL-1β, IL-2, and IL-6 showed temporal fluctuations, including decreases at intermediate time points followed by partial recovery. Overall, these results indicate that BCG vaccination induced distinct temporal patterns of immune gene expression in the spleen and lung, with more pronounced changes observed in the lung at week 8.

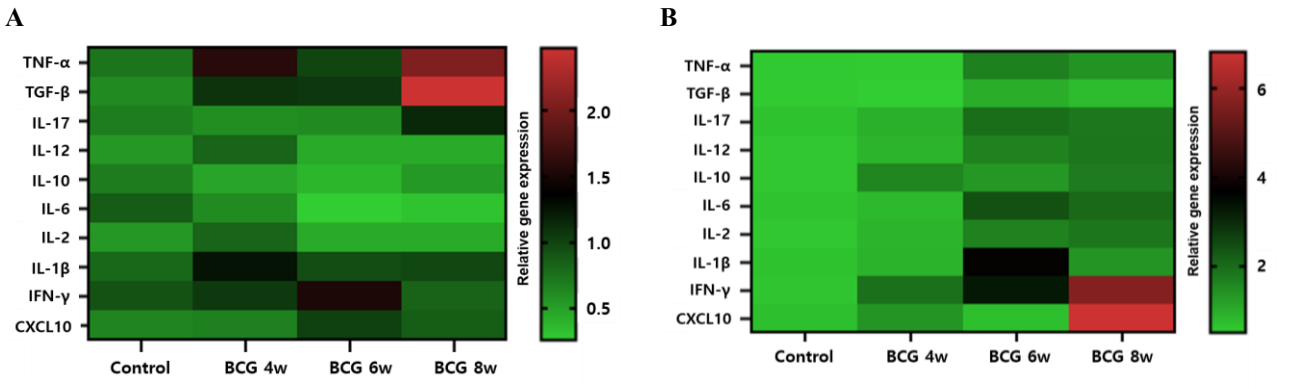

Fig. 5: Heatmap of immune-related gene expression patterns in the spleen and lung. Heatmap showing the relative expression of cytokine and chemokine-related genes in the control and BCG 4, 6, and 8 weeks groups. Gene expression patterns are presented for the (A) spleen and (B) lung tissue. The color scales indicate the relative expression levels of the genes.

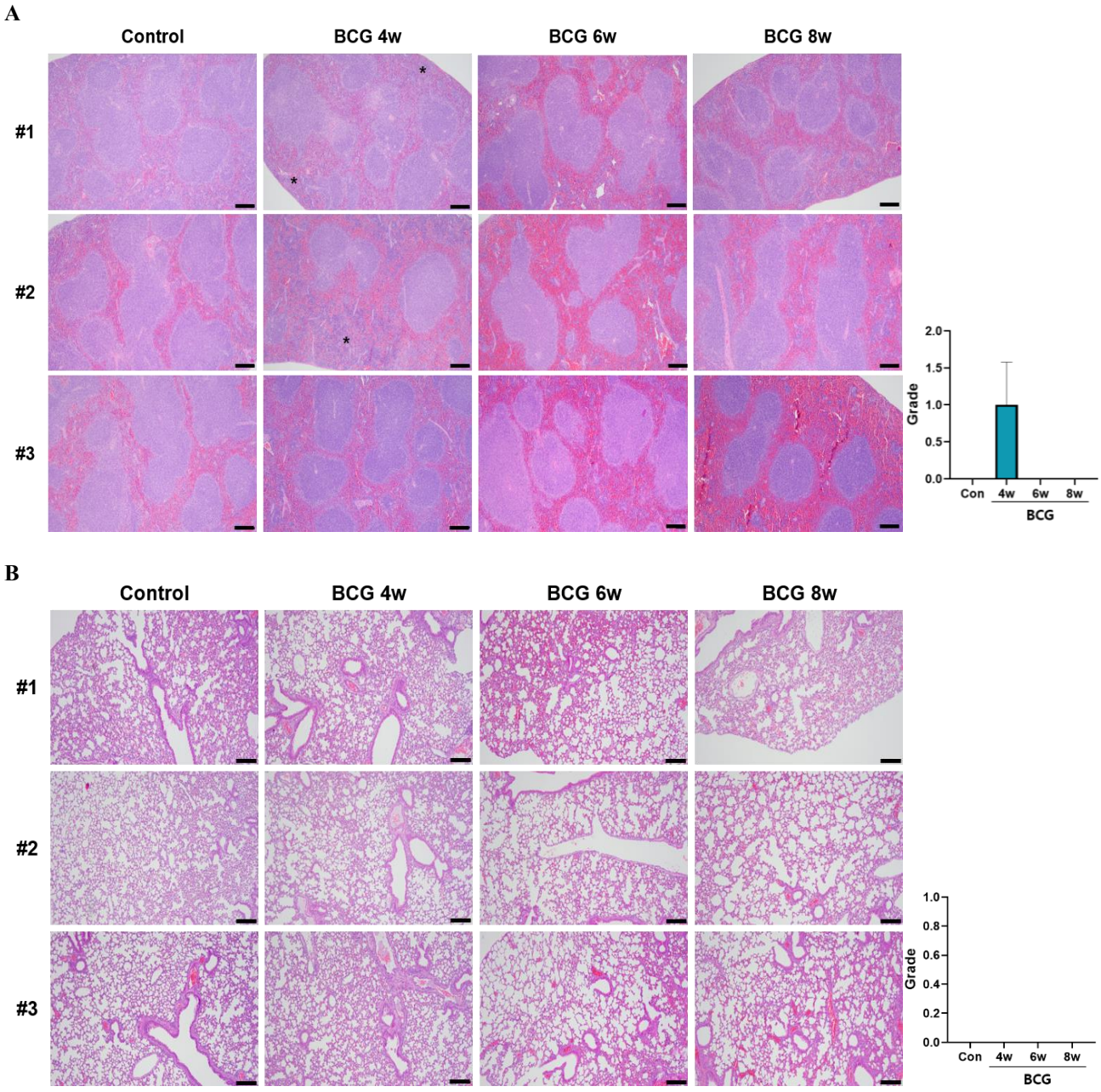

Fig. 6: Histopathological analysis of spleen and lung tissue. Hematoxylin and eosin staining was done to assess inflammatory and structural changes. (A) In spleen tissue, mild cellular infiltration and red pulp expansion were observed in a subset of vaccinated mice. (B) Lung tissue retained a normal morphology at all time points. Quantification was performed using ImageJ and expressed as the percentage of positively stained area. Data are presented as the mean ± SEM (n=3). Magnification × 100, Scale bar = 200 µm. *: increased infiltration of mixed inflammatory cells.

Histopathological Changes Remain Minimal Despite Increasing Immune Activation: Histological analysis revealed that BCG vaccination did not induce overt inflammatory pathology. Lung tissues retained a normal architecture at all time points (Fig. 6B), and only minor immune-cell infiltration was observed in the spleen of vaccinated mice (Fig. 6A). Importantly, no evidence of tissue disruption or excessive inflammation was observed, which indicates that immune activation was regulated, rather than pathological.

Tissue-Localized Cytokine Signaling Intensifies at Later Time Points: IHC analysis revealed increased expression of cytokine-positive cells, most prominently at week 8. In spleen tissue, IL-2 (3.51 at 8w; P=0.018) exhibited the largest increase (Fig. 7), whereas TNF-α (23.02 at 8w; P=0.006) expression in lung sections increased significantly at the final time point (Fig. 8). The results suggest progressive localization of immune signaling within key immunological organs during the later phases of vaccine-induced immunity.

Effect of BCG Vaccination Duration on Pulmonary Bacterial Burden Following Infection: Following aerosol challenge with M.tb, the bacterial burden in the spleen and lung was evaluated at multiple time points to compare the effects of different BCG vaccination intervals. In the spleen, CFU levels remained relatively low in most groups throughout the observation period, whereas no statistically significant differences were observed among the vaccination groups (Fig. 9A). Although the 8-week (34.63×10^3; P<0.001) vaccination group showed a higher splenic bacterial burden at DPI 42, this increase was not statistically significant. By DPI 56, splenic CFU levels were again relatively low and comparable among the groups. In the lung, the bacterial burden differed according to the interval between BCG vaccination and aerosol challenge (Fig. 9B). At DPI 28, the 4 weeks vaccination group (20.8×10^4) showed the lowest pulmonary CFU level, whereas higher bacterial burdens were observed in the 6 (52.23×10^4; P<0.001) and 8 (53.17×10^4; P<0.001) week groups. At DPI 42, the 8 weeks vaccination group (37.43×10^4; P=0.012) exhibited the lowest pulmonary bacterial burden among the vaccinated groups, whereas the 4 (48.95×10^4; P=0.007) and 6 (50.27×10^4; P=0.001) week groups showed similar CFU levels. A similar pattern was observed at DPI 56, with the lowest lung CFU level observed in the 8 weeks group (18.3×10^4), followed by the 4 (27.93×10^4) and 6 (43.15×10^4; P=0.011) week groups. These results indicate that the effects of BCG vaccination duration on bacterial control differed between the spleen and lung and varied based on the post-infection time point.

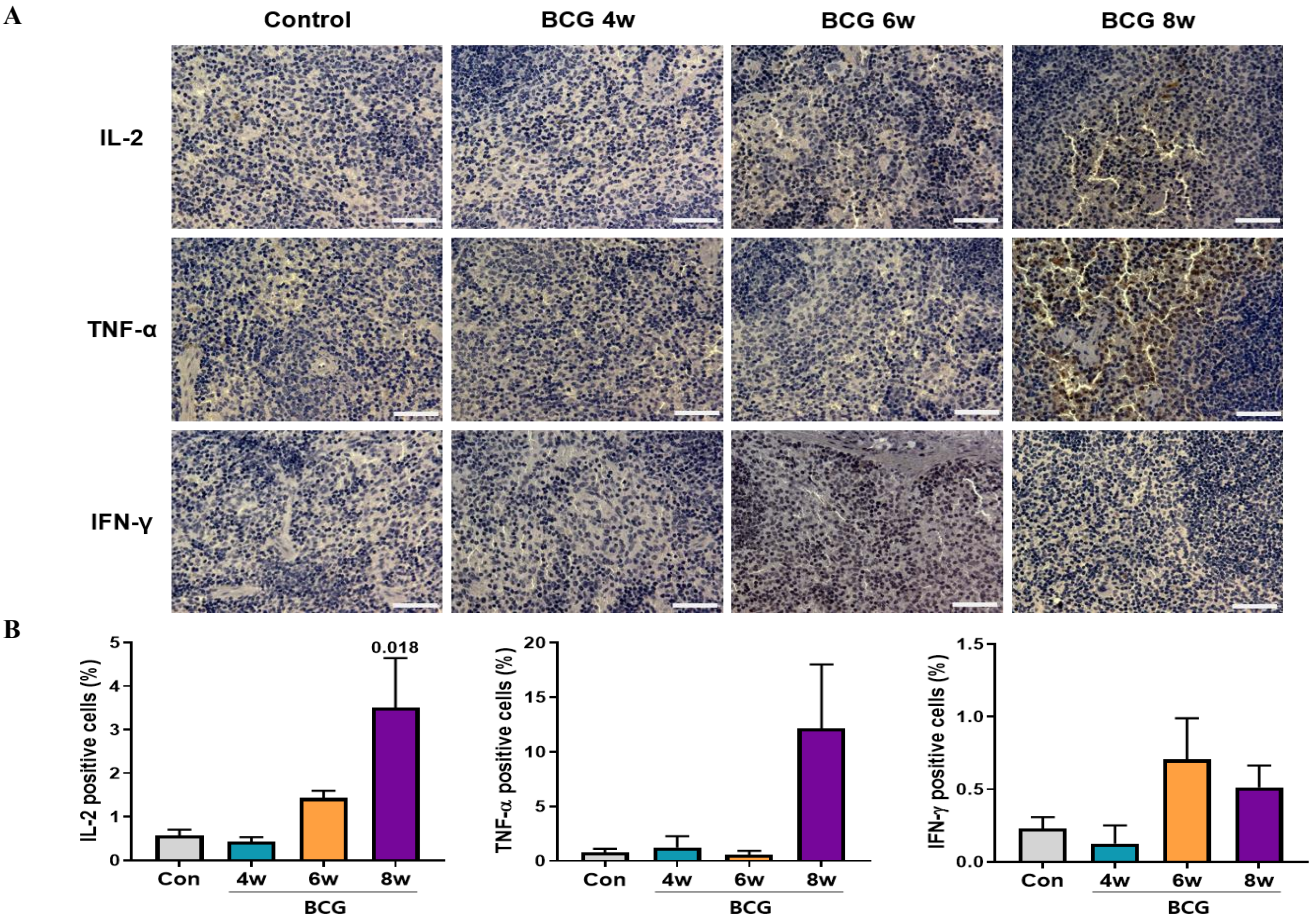

Fig. 7: Immunohistochemical (IHC) detection of immune markers in the spleen. (A) Representative IHC images of IL-2, TNF-α, and IFN-γ expression in spleen tissues from the control and BCG 4, 6, and 8 weeks groups. Columns represent experimental groups, and rows represent the staining targets, IL-2, TNF-α, and IFN-γ. (B) Quantification of the positively stained area using ImageJ software, expressed as the percentage of the positively stained area. Data are presented as the mean ± SEM (n=3). Statistical analysis was performed using a one-way ANOVA followed by Dunnett's multiple comparisons test, with each BCG-vaccinated group compared with the control group. Exact adjusted *P* values are shown in the figure. Scale bar = 100 μm.

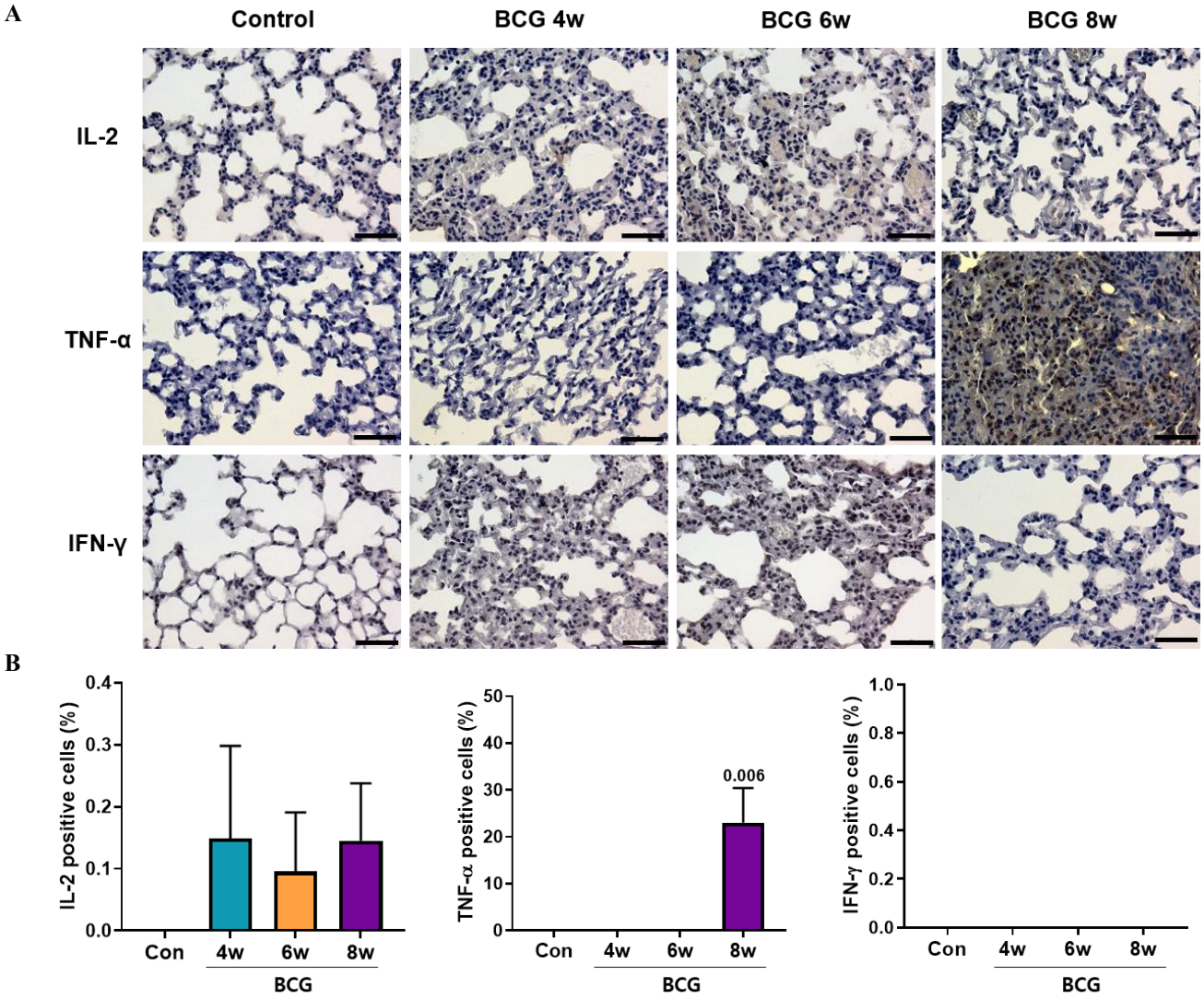

Fig. 8: Immunohistochemical (IHC) detection of immune markers in the lung. (A) Representative IHC images of IL-2, TNF-α, and IFN-γ expression in lung tissues from the control and BCG 4, 6, and 8 weeks groups. Columns represent experimental groups, and rows represent the staining targets, IL-2, TNF-α, and IFN-γ. (B) Quantification of the positively stained area using ImageJ software, expressed as a percentage of the positively stained area. Data are presented as the mean ± SEM (n=3). Statistical analysis was performed using a one-way ANOVA followed by Dunnett's multiple comparisons test, with each BCG-vaccinated group compared with the control group. Exact adjusted P values are shown in the figure. Scale bar = 100 μm.

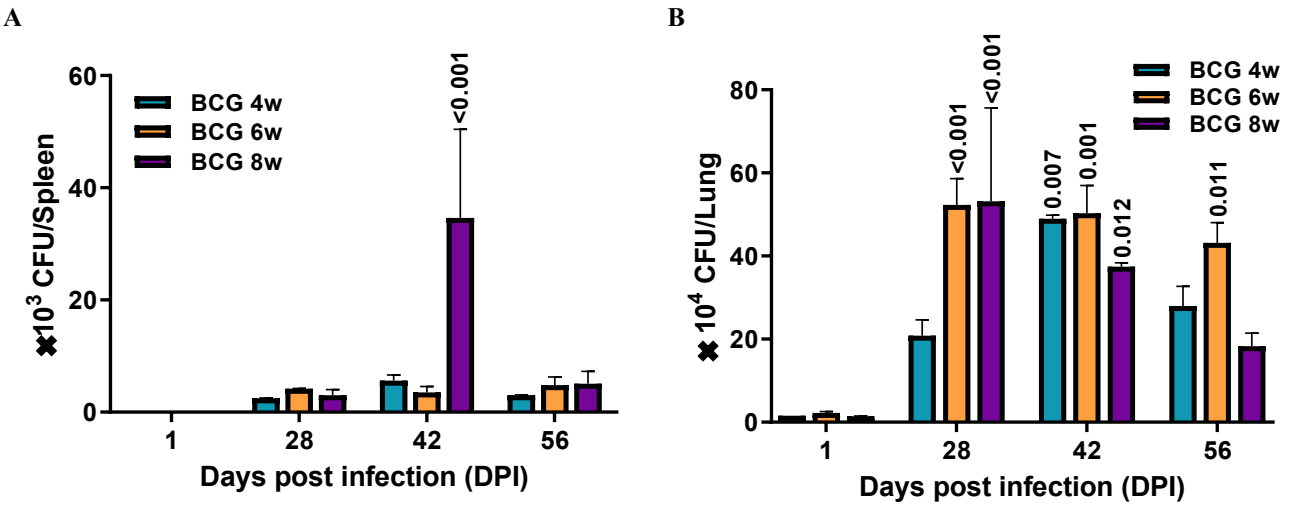

Fig. 9: Effect of BCG vaccination duration on bacterial burden in the spleen and lung following aerosol challenge with *Mycobacterium tuberculosis* (M.tb). C57BL/6 mice were vaccinated with BCG 4, 6, or 8 weeks before aerosol challenge with M.tb H37Rv. (A) Spleen and (B) lung tissues were collected at DPI 1, 28, 42, and 56, and bacterial burden was determined by CFU enumeration. The data are presented as the mean ± SEM (n=3). Statistical analysis was performed using a one-way ANOVA followed by Dunnett's multiple comparisons test, with each post-infection time point compared with DPI 1 within the corresponding vaccination group. Exact adjusted *P* values are shown in the figure.

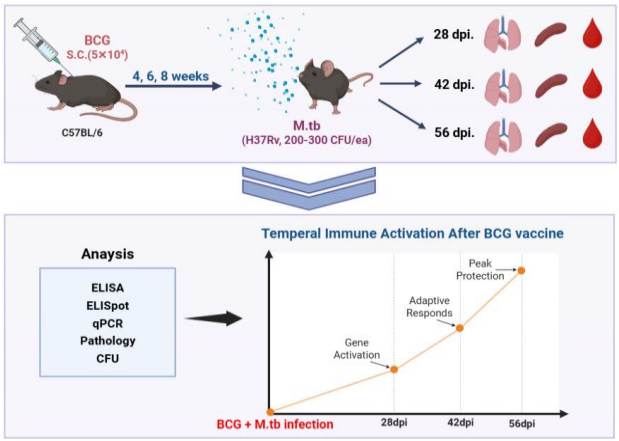

Fig. 10: Schematic representation of temporal immune activation following BCG vaccination. The diagram illustrates the progressive development of immune responses over time following a single subcutaneous BCG dose. Initial exposure (week 0; control) triggers early immune priming, followed by increases in cytokine production and transcriptional activation around week 4. A marked enhancement in adaptive immune activity, including elevated Th1-associated responses, occurs by week 6. By week 8, immune activation peaks, corresponding to enhanced immune activation and improved protection outcomes. This conceptual framework summarizes the coordinated progression from vaccination to functional protection. Created in BioRender. Kim, W. (2025) https://BioRender.com/o05whx1.

DISCUSSION

In this study, we examined the temporal dynamics of immune responses to BCG vaccination in C57BL/6 mice through the analysis of immunological changes at 4, 6, and 8 weeks following vaccination. Initially, quantitative PCR indicated that spleen tissues had a marked upregulation of cytokine and chemokine transcripts (Fig. 4A). A notable finding was a statistically significant increase in IFN-γ expression observed at 8 weeks following vaccination (Fig. 4A), suggesting a strong Th1-skewed immune response (Nakagome *et al.*, 2009). The increased expression of CXCL10 suggests a potential inclination toward promoting Th1 polarization (Zou *et al.*, 2025). The concurrent increases in IL-12, IFN-γ, and CXCL10 may reflect the development of a Th1-associated pulmonary immune environment. IL-12 promotes the activation of Th1 and natural killer cells and promotes IFN-γ production (Trinchieri, 1995; Narinyan *et al.*, 2022), whereas IFN-γ induces CXCL10 expression and promotes the recruitment of activated immune cells (Lande *et al.*, 2003).

In contrast to pulmonary Th1-associated changes, splenic IL-10 expression was decreased throughout the vaccination period and was significantly reduced at weeks 6 and 8 (Fig. 4A). Because IL-10 exerts regulatory effects by limiting macrophage activation and pro-inflammatory cytokine production (Lei *et al.*, 2024), this reduction may be consistent with decreased regulatory activity in the systemic immune compartment (Lei *et al.*, 2024); however, these expression patterns alone do not indicate that reduced splenic IL-10 directly caused the increases in pulmonary Th1-associated mediators (Jeevan *et al.*, 2009). IL-6 and IL-10 exhibited distinct tissue-specific temporal patterns (Gunasena *et al.*, 2022). In the spleen, IL-6 initially decreased, but partially recovered by week 8 (Fig. 4A). In contrast, pulmonary IL-6 exhibited an increasing tendency at later time points, although the differences were not statistically significant (Fig. 4B). Splenic IL-10 decreased over time (Fig. 4A), whereas pulmonary IL-10 exhibited variable changes, with higher mean expression at weeks 4 and 8, but no statistically significant differences among the groups (Fig. 4B). These results indicate that IL-6 and IL-10 have distinct tissue-specific expression patterns following BCG vaccination. Various inflammatory mediators, including IL-1β and IL-2, showed temporal fluctuations, whereas IL-17, IL-12, and TNF-α exhibited a modest but consistent increase throughout the study. Because IL-1β contributes to the initiation of innate inflammatory responses (Netea *et al.*, 2010), its transient reduction and subsequent recovery may reflect time-dependent regulation of inflammatory activity following BCG vaccination, rather than sustained inflammatory activation; however, as IL-1β protein secretion and inflammasome activity were not directly evaluated, the biological significance of this transcriptional pattern remains unclear. Although, splenic gene expression exhibited more modest and temporally restricted changes compared with lung tissue, aside from TNF-α and TGF-β, which exhibited a mild increase at 8 weeks (Fig. 4A, 5A). These results suggest that the overall transcriptional changes were more pronounced in the lung than in the spleen, although IL-6 and IL-10 showed distinct tissue-specific temporal patterns (Fig. 4, 5). The divergent temporal responses between the spleen and lung may reflect compartmentalization of BCG-induced immunity (Fulton *et al.*, 2000; Silver *et al.*, 2023). The early splenic response may indicate transient systemic expansion of activated lymphocytes, followed by contraction of the peripheral response. In contrast, continued pulmonary transcriptional activation may result from the recruitment and retention of activated immune cells in the lung, and the gradual establishment of local memory populations (Perdomo *et al.*, 2016).

BCG induces trained immunity through long-lasting functional reprogramming of innate immune cells, which results in enhanced secondary responses (Netea *et al.*, 2016). This mechanism may contribute in part to the sustained systemic and tissue-level immune activation observed at later time points. The sustained pulmonary transcriptional response may also be related to the establishment or retention of lung-resident memory T cells, which provide rapid local cytokine responses upon respiratory exposure (Wu *et al.*, 2021); however, the contributions of trained immunity and lung-resident memory T-cell populations to these tissue-specific temporal responses remain unclear.

A correlation analysis conducted among cytokine genes indicated a significant association within pulmonary tissue, specifically between TNF-α and TGF-β, IL-17, and IL-6. This indicates that the expression profile of these mediators changed across the experimental groups but did not establish direct regulatory interactions or a functional immune network. This suggests a coordinated regulation among pro-inflammatory and regulatory cytokines within the local tissue microenvironment (Martinez *et al.*, 2008). Moreover, IL-2, IL-12, and IL-6 exhibited significant correlations, indicating the potential for co-regulation of important mediators associated with the Th1/Th17 response

(Martinez *et al.*, 2008). A significant relationship was observed in the spleen between the expression of IL-2 and IL-12 (Fig. 4A, 5A), suggesting an association between their temporal expression patterns, despite the relatively limited splenic transcriptional response (Gollob *et al.*, 1999; Lai *et al.*, 2023). The examination of serum cytokine levels revealed the progression of systemic immune activation over time. IFN-γ and IL-2 levels exhibited a significant increase by week 8 (Fig. 2A, B), which supports the results of transcriptomic analysis and suggests a continued Th1 immune response at the protein level (Martinez*, et al.*, 2008). TNF-α exhibited mild temporal fluctuations without statistically significant differences (Fig. 2C), suggesting that systemic TNF-α levels remained relatively stable following BCG vaccination. The apparent discrepancy between systemic and tissue-level TNF-α responses suggests that TNF-α regulation following BCG vaccination is primarily localized rather than systemic (Ly and McMurray, 2009), which highlights compartment-specific immune modulation.

The apparent divergence between the week 4 peak in the splenic IFN-γ ELISpot response and the week 8 peak in serum IFN-γ indicates differences in the biological compartment and assay endpoint rather than conflicting results (Fig. 3C). The ELISpot assay quantified PPD-responsive splenocytes capable of secreting IFN-γ following ex vivo antigen stimulation, whereas serum ELISA measured the circulating IFN-γ concentration at the time of sampling without antigen-specific stimulation (Lalvani, 2007). Thus, ELISpot reflects the frequency of antigen-responsive IFN-γ–secreting cells within the spleen, whereas serum ELISA reflects the systemic cytokine milieu arising from multiple cell and tissue sources (Hagen *et al.*, 2015). Consistent with the compartmentalized temporal response described above, the early splenic ELISpot peak may represent initial expansion followed by contraction of the splenic cellular response (Kamath *et al.*, 2000), whereas the subsequent serum peak is consistent with continued systemic and tissue-associated immune activation (Pedras-Vasconcelos *et al.*, 2002). The late increases in splenic and pulmonary IFN-γ and CXCL10 mRNA expression further support persistent tissue-associated immune activation at week 8, but do not establish a cellular source for circulating IFN-γ. Accordingly, the ELISpot and ELISA results should be considered complementary rather than contradictory. Because immune-cell phenotypes and cellular trafficking were not directly evaluated, this mechanistic interpretation is provisional.

The histopathological analysis revealed the absence of inflammatory damage in the lung, indicating that immune activation triggered by BCG does not result in harmful tissue changes in the pulmonary region (Fig. 6B). In the spleen, a limited number of animals showed slight necrosis and inflammatory infiltration in the red pulp, whereas the majority of tissues maintained typical histoarchitecture (Fig. 6A). These results indicate that immune activation occurred within normal physiological parameters, without causing overt pathological inflammation (Sun *et al.*, 2015). IHC staining revealed notable temporal increases in IL-2 expression in splenic tissue (Fig. 7B), consistent with systemic cytokine profiles and supporting localized T-cell activation (Mollenkopf *et al.*, 2004; Kaveh *et al.*, 2014). Although TNF-α, IFN-γ, and mycobacterial antigens exhibited upward trends, statistical significance was not achieved (Fig. 7B); however, the observed patterns indicate a gradual immunological response at the tissue level over 8 weeks. These results suggest that the decrease in IL-10, together with the increases in IL-12, IFN-γ, and CXCL10, reflects a shift toward a Th1-associated immune response following BCG vaccination (Pitt *et al.*, 2012). The temporary reduction and later recovery of IL-1β indicate time-dependent regulation of innate inflammatory activity.

Taken together, these results indicate that BCG vaccination in C57BL/6 mice induces distinct temporal patterns of systemic and tissue-specific immune activation, rather than a uniform progressive response. The significant increase in Th1-related markers, such as IFN-γ and IL-2, at the levels of gene and protein expression highlights the vaccine's capacity to induce robust cellular immune responses (Kaveh *et al.*, 2014; Kleinnijenhuis *et al.*, 2014). In addition, the varying rates of immune activation in different tissues underscore the significance of selecting suitable time intervals and biological measurements when assessing the effectiveness of vaccines and the development of immune memory (Uranga *et al.*, 2016; Woodworth *et al.*, 2021). This study offers significant insight into the timing and mechanisms involved, which may contribute to improving BCG-based immunization strategies and advancing the development of future vaccines. The integrated temporal changes in systemic and tissue-specific immune responses following BCG vaccination and subsequent M.tb challenge are summarized in Fig. 10.

Conclusions: This study provides temporal insight into immune responses following BCG vaccination. These results contribute to the selection of appropriate time points and key immunological parameters for future studies evaluating vaccine immunogenicity and efficacy. Furthermore, the insights gained from this study may enable optimization of BCG-based immunization strategies and support the development of next-generation vaccines.

Authors contribution: E.B.C. and Y.J.Y. performed the experiments and drafted the manuscript. K.W.K. and S.Y.M. analyzed the sera and tissue samples. H.J.L and Y.K.L contributed to data analysis and visualization. I.O.O. and K.I.P. served as co-corresponding authors and designed and supervised the study. All authors interpreted the data, revised the manuscript, and approved the final version.

Funding: This study received financial support from the Korea Disease Control and Prevention Agency (KDCA; 6600-6634-313) and from the National Research Foundation of Korea (NRF) Basic Science Research Program funded by the Ministry of Education (RS-2022-NR075631).

REFERENCES

Bickett TE, McLean J, Creissen E, *et al.*, 2020. Characterizing the BCG induced macrophage and neutrophil mechanisms for defense against *Mycobacterium tuberculosis*. Frontiers in Immunology 11:1202.

Bussi C and Gutierrez MG, 2019. *Mycobacterium tuberculosis* infection of host cells in space and time. FEMS Microbiology Reviews 43:341-61.

Chee CBE, Reves R, Zhang Y, *et al.*, 2018. Latent tuberculosis infection: Opportunities and challenges. Respirology 23:893-900.

Chen J, Gao L, Wu X, *et al.*, 2023. BCG-induced trained immunity: history, mechanisms and potential applications. Journal of Translational Medicine 21:106.

Cho T, Khatchadourian C, Nguyen H, *et al.*, 2021. A review of the BCG vaccine and other approaches toward tuberculosis eradication. Human Vaccines & Immunotherapeutics 17:2454-70.

Coppola M, Jurion F, van den Eeden SJF, *et al.*, 2021. In-vivo expressed *Mycobacterium tuberculosis* antigens recognised in three mouse strains after infection and BCG vaccination. NPJ Vaccines 6:81.

Covian C, Fernandez-Fierro A, Retamal-Diaz A, *et al.*, 2019. BCG-Induced Cross-Protection and Development of Trained Immunity: Implication for Vaccine Design. Frontiers in Immunology 10:2806.

Fatima S, Kumari A, Das G, *et al.*, 2020. Tuberculosis vaccine: A journey from BCG to present. Life Sciences 252:117594.

Foster M, Hill PC, Setiabudiawan TP, *et al.*, 2021. BCG-induced protection against *Mycobacterium tuberculosis* infection: Evidence, mechanisms, and implications for next-generation vaccines. Immunological Reviews 301:122-44.

Fulton SA, Martin TD, Redline RW, *et al.*, 2000. Pulmonary immune responses during primary *Mycobacterium bovis*- Calmette-Guerin bacillus infection in C57Bl/6 mice. American Journal of Respiratory Cell and Molecular Biology 22:333-43.

Furin J, Cox H and Pai M, 2019. Tuberculosis. The Lancet 393:1642-56.

Gollob JA, Schnipper CP, Murphy EA, *et al.*, 1999. The functional synergy between IL-12 and IL-2 involves p38 mitogen-activated protein kinase and is associated with the augmentation of STAT serine phosphorylation. The Journal of Immunology 162:4472-81.

Gunasena M, Shukla RK, Yao N, *et al.*, 2022. Evaluation of early innate and adaptive immune responses to the TB vaccine *Mycobacterium bovis* BCG and vaccine candidate BCGDeltaBCG1419c. Scientific Reports 12:12377.

Hagen J, Zimmerman R, Goetz C, *et al.*, 2015. Comparative multi-donor study of IFNgamma secretion and expression by human PBMCs using ELISPOT side-by-side with ELISA and Flow Cytometry Assays. Cells 4:84-95.

Jeevan A, Bonilla DL and McMurray DN, 2009. Expression of interferon-gamma and tumour necrosis factor-alpha messenger RNA does not correlate with protection in guinea pigs challenged with virulent Mycobacterium tuberculosis by the respiratory route. Immunology 128:e296-305.

Kamath AT, Groat NL, Bean AG, *et al.*, 2000. Protective effect of DNA immunization against mycobacterial infection is associated with the early emergence of interferon-gamma (IFN-gamma)-secreting lymphocytes. Clinical and Experimental Immunology 120:476-82.

Kaveh DA, Garcia-Pelayo MC and Hogarth PJ, 2014. Persistent BCG bacilli perpetuate CD4 T effector memory and optimal protection against tuberculosis. Vaccine 32:6911-8.

Khatri B, Keeble J, Dagg B, *et al.*, 2021. Efficacy and immunogenicity of different BCG doses in BALB/c and CB6F1 mice when challenged with H37Rv or Beijing HN878. Scientific Reports 11:23308.

Kleinnijenhuis J, Quintin J, Preijers F, *et al.*, 2014. Long-lasting effects of BCG vaccination on both heterologous Th1/Th17 responses and innate trained immunity. Journal of Innate Immunity 6:152-8.

Kowalewicz-Kulbat M and Locht C, 2021. BCG for the prevention and treatment of allergic asthma. Vaccine 39:7341-52.

Kramnik I and Beamer G, 2016. Mouse models of human TB pathology: roles in the analysis of necrosis and the development of host-directed therapies. Seminars in Immunopathology 38:221-37.

Lai R, Gong DN, Williams T, *et al.*, 2023. Host genetic background is a barrier to broadly effective vaccine-mediated protection against tuberculosis. The Journal of Clinical Investigation 133(13):e167762.

Lalvani A, 2007. Diagnosing tuberculosis infection in the 21st century: new tools to tackle an old enemy. Chest 131:1898-906.

Lande R, Giacomini E, Grassi T, *et al.*, 2003. IFN-alpha beta released by *Mycobacterium tuberculosis*-infected human dendritic cells induces the expression of CXCL10: selective recruitment of NK and activated T cells. The Journal of Immunology 170:1174-82.

Lei Q, Fu H, Yao Z, *et al.*, 2024. Early introduction of IL-10 weakens BCG revaccination's protection by suppressing CD4(+)Th1 cell responses. Journal of Translational Medicine 22:1103.

Ly LH and McMurray DN, 2009. The Yin-Yang of TNFalpha in the guinea pig model of tuberculosis. Indian Journal of Experimental Biology 47:432-9.

Lyon SM and Rossman MD, 2017. Pulmonary Tuberculosis. Microbiology Spectrum 5:

Martinez GJ, Nurieva RI, Yang XO, *et al.*, 2008. Regulation and function of proinflammatory TH17 cells. Annals of the New York Academy of Sciences 1143:188-211.

Mata E, Tarancon R, Guerrero C, *et al.*, 2021. Pulmonary BCG induces lung-resident macrophage activation and confers long-term protection against tuberculosis. Science Immunology 6:eabc2934.

Mollenkopf HJ, Kursar M and Kaufmann SH, 2004. Immune response to postprimary tuberculosis in mice: *Mycobacterium tuberculosis* and *Mycobacterium bovis* bacille Calmette-Guerin induce equal protection. The Journal of Infectious Diseases 190:588-97.

Nakagome K, Okunishi K, Imamura M, *et al.*, 2009. IFN-gamma attenuates antigen-induced overall immune response in the airway as a Th1-type immune regulatory cytokine. The Journal of Immunology 183:209-20.

Narinyan W, Poladian N, Orujyan D, *et al.*, 2022. Immunologic Role of Innate Lymphoid Cells against Mycobacterial tuberculosis Infection. Biomedicines 10(11):2828.

Netea MG, Joosten LA, Latz E, *et al.*, 2016. Trained immunity: A program of innate immune memory in health and disease. Science 352:aaf1098.

Netea MG, Simon A, van de Veerdonk F, *et al.*, 2010. IL-1beta processing in host defense: beyond the inflammasomes. PLOS Pathogens 6:e1000661.

Pedras-Vasconcelos JA, Chapdelaine Y, Dudani R, *et al.*, 2002. *Mycobacterium bovis* BCG-infected mice are more susceptible to staphylococcal enterotoxin B-mediated toxic shock than uninfected mice despite reduced in vitro splenocyte responses to superantigens. Infection and Immunity 70:4148-57.

Perdomo C, Zedler U, Kuhl AA, *et al.*, 2016. Mucosal BCG vaccination induces protective lung-resident memory T cell populations against Tuberculosis. mBio 7:

Pitt JM, Stavropoulos E, Redford PS, *et al.*, 2012. Blockade of IL-10 signaling during Bacillus Calmette-Guerin vaccination enhances and sustains Th1, Th17, and innate lymphoid IFN-gamma and IL-17 responses and increases protection to Mycobacterium tuberculosis infection. The Journal of Immunology 189:4079-87.

Ritz N, Hanekom WA, Robins-Browne R, *et al.*, 2008. Influence of BCG vaccine strain on the immune response and protection against tuberculosis. FEMS Microbiology Reviews 32:821-41.

Sankar P and Mishra BB, 2023. Early innate cell interactions with *Mycobacterium tuberculosis* in protection and pathology of tuberculosis. Frontiers in Immunology 14:1260859.

Sawyer AJ, Patrick E, Edwards J, *et al.*, 2023. Spatial mapping reveals granuloma diversity and histopathological superstructure in human tuberculosis. Journal of Experimental Medicine 220(6):e20221392.

Silver RF, Xia M, Storer CE, *et al.*, 2023. Distinct gene expression signatures comparing latent tuberculosis infection with different routes of Bacillus Calmette-Guerin vaccination. Nature Communications 14:8507.

Suarez I, Funger SM, Kroger S, *et al.*, 2019. The diagnosis and treatment of Tuberculosis. Deutsches Ärzteblatt International 116:729-35.

Sun W, Meng K, Qi C, *et al.*, 2015. Immune-enhancing activity of polysaccharides isolated from Atractylodis macrocephalae Koidz. Carbohydrate Polymers 126:91-6.

Trinchieri G, 1995. Interleukin-12: a proinflammatory cytokine with immunoregulatory functions that bridge innate resistance and antigen-specific adaptive immunity. Annual Review of Immunology 13:251-76.

Uranga S, Marinova D, Martin C, *et al.*, 2016. Protective efficacy and pulmonary immune response following subcutaneous and intranasal BCG administration in mice. Journal of Visualized Experiments 115:e54440.

Warner DF, Barczak AK, Gutierrez MG, *et al.*, 2025. *Mycobacterium tuberculosis* biology, pathogenicity and interaction with the host. Nature Reviews Microbiology 23:788-804.

Woodworth JS, Clemmensen HS, Battey H, *et al.*, 2021. A *Mycobacterium tuberculosis*-specific subunit vaccine that provides synergistic immunity upon co-administration with Bacillus Calmette-Guerin. Nature Communications 12:6658.

Wu Q, Kang S, Huang J, *et al.*, 2021. Antigen-specific tissue-resident memory T cells in the respiratory system were generated following intranasal vaccination of mice with BCG. Journal of Immunology Research 2021:6660379.

Zhu L, Yang Q, Ding S, *et al.*, 2026. TCF21 mediates ITGA8 to block LUAD progression and immune escape. Molecular & Cellular Toxicology 22(1):31-45.

Zou Y, Huang F, Sun J, *et al.*, 2025. The role of IFN-gamma/CXCL10 axis in Mycoplasma pneumonia infection. Scientific Reports 15(1):2671.